Effect of knotting on polymer shapes and their enveloping ellipsoids

Kenneth C. Millett,[1,a)] Patrick Plunkett,[1,b)] Michael Piatek,[2,c)] Eric J. Rawdon,[3,d)] and Andrzej Stasiak[4,e)]
[1]*Department of Mathematics, University of California, Santa Barbara, Santa Barbara, California 93106, USA*
[2]*Department of Computer Science and Engineering, University of Washington, Seattle, Washington 98195, USA*
[3]*Department of Mathematics, University of St. Thomas, St. Paul, Minnesota 55105, USA*
[4]*Faculty of Biology and Medicine, Center for Integrative Genomics, University of Lausanne, Lausanne CH 1015, Switzerland*

(Received 21 January 2009; accepted 23 March 2009; published online 24 April 2009)

We simulate freely jointed chains to investigate how knotting affects the overall shapes of freely fluctuating circular polymeric chains. To characterize the shapes of knotted polygons, we construct enveloping ellipsoids that minimize volume while containing the entire polygon. The lengths of the three principal axes of the enveloping ellipsoids are used to define universal size and shape descriptors analogous to the squared radius of gyration and the inertial asphericity and prolateness. We observe that polymeric chains forming more complex knots are more spherical and also more prolate than chains forming less complex knots with the same number of edges. We compare the shape measures, determined by the enveloping ellipsoids, with those based on constructing inertial ellipsoids and explain the differences between these two measures of polymer shape.
 [DOI: 10.1063/1.3117923]

I. INTRODUCTION

Polymer chains in Θ conditions have long been modeled as freely jointed random isosegmental polygons that can freely change their spatial position. Such representations of polymeric molecules are a consequence of their statistical properties under Θ conditions where independent segments of the polymer chains neither attract nor repel each other. Many aspects of the physical properties and the associated biological activity of linear, branched, and ring polymers under Θ conditions are relatively well understood and have been extensively explored, both theoretically and through numerical simulations. For ring polymers, however, the behavior of these properties becomes more complex when the topology of the ring is taken into account. The presence of knots in polymers has been considered from several perspectives[1–7] leading to an appreciation for the importance of their influence on the properties of polymers. In particular, a substantial number of studies have considered how different properties of circular molecules depend on the specific knot type of the macromolecule and how they relate to those of the phantom polymers, i.e., the average over all polymers.[8–16] In this research, we focus attention on measures of the size and shape of the enveloping ellipsoids of ring polymers and the influence of knotting on measures of these shapes.

Kuhn[17] proposed that for entropic reasons, the overall shape of momentary random coils formed by polymer chains at thermodynamic equilibrium should resemble prolate ellipsoids rather than spheres. His observation was confirmed in both numerical studies and experiments.[18–27] Proteins have also been modeled by anisotropic ellipsoidal shapes known as inertial, momental, or Cauchy ellipsoids[28,29] having the same inertial properties as the corresponding proteins. A numerical measure of this anisotropy, the *asphericity*, is derived from the eigenvalues of the inertial tensor associated to a frozen momentary configuration adopted by the polymer chain.[30] The mean asphericity has been applied widely to measure the extent to which random chains and ring polygons deviate from a spherical shape.[31–33] By replacing the eigenvalues in the definition of asphericity with the square root of three times the eigenvalues, we showed that one can define an unbiased system of measures of scale and shape.[16] We used this system to measure the impact of knotting on the average inertial shape of frozen momentary configurations of circular polymer chains with increasing length. The inertial measures bring together the distance from the center of mass and the density of the polymer in their measure of shape. Thus, although external portions of the polymer contribute to this characterization, one might ask if there would be a different sense of shape if one were to consider a "hard barrier" surrounding the polymer.

To respond to this question, we identify the smallest ellipsoid, in terms of volume, containing the entire polymer using an algorithm developed by Schonherr.[34] In their study of diffusion of proteins in solution, Ryabov *et al.*[27] employed a more complex method to define an enveloping ellipsoid of a protein in which they first use software that identifies the protein surface exposed to solvent molecules of a given radius (see also Ref. 35). They then use a principal component

[a)]Electronic mail: millett@math.ucsb.edu.
[b)]Electronic mail: plunkett@math.ucsb.edu.
[c)]Electronic mail: piatek@cs.washington.edu.
[d)]Author to whom correspondence should be addressed. Electronic mail: ejrawdon@stthomas.edu.
[e)]Electronic mail: andrzej.stasiak@unil.ch.

analysis to identify the axes and dimensions of an ellipsoid. They note that diffusion characteristics are important factors in limiting reactions and in the interpretation of data from experiments involving proteins in solutions. The anisotropy of such enveloping ellipsoids has proven to be important at all physical scales, from the astronomical[36] to that of dendrimer macromolecules[37] and metal organic molecules in vapor absorption on polymer host lattices.[38] These enveloping ellipsoids capture critical properties of the objects. Ellipsoidal shapes now find applications in the synthesis and chemical analysis of nanomaterials such as endohedral metallofullerene cages.[39]

In this study of the influence of knotting on shape, we use the semiaxis lengths of the enveloping ellipsoids in the formulae for the asphericity (formula 2) and prolateness (formula 3) employed earlier in the inertial setting.[16] We call the resulting numerical measures the *enveloping asphericity* and *enveloping prolateness* to distinguish them from the analogous measures derived from the moment of inertia tensor. To complete the comparison of scale and shape for the enveloping ellipsoids, we define a quantity analogous to the squared radius of gyration. This new quantity is defined to be one-third the sum of the squared semiaxis lengths (formula 1).

Analysis of collections of freely jointed random isosegmental polygons across the range of 6–500 edges shows that more complex knots are, from the perspective of enveloping measures, more spherical and more prolate than chains forming less complex knots for the same number of segments. We compare and explain the differences between the shape characterizations arising from the inertial ellipsoid and those defined by the enveloping ellipsoid measures of polymer shape across the range of lengths in our study.

II. MEASURES OF SIZE AND SHAPE

In Ref. 16, we employed three measures of size and shape derived from the moment of inertia tensor. The first was the squared radius of gyration R^2 given in formula 1 in terms of the semiaxis lengths, a, b, and c, of the associated characteristic inertial ellipsoid defined in Ref. 16. The second was a measure of asphericity A given in formula 2.[30,40] The third was the prolateness (also known as the nature of asphericity) P given in formula 3 as defined by Aronovitz and co-workers.[40,41]

To determine the enveloping asphericity, one first finds the ellipsoid of smallest volume containing the modeled polymer. The semiaxis lengths a, b, and c of that ellipsoid are then substituted in formulas 1–3. In short, we replace the characteristic inertial ellipsoid by the enveloping ellipsoid in the definitions of the R^2, A, and P. Using these measures, we determine their average values for the entire (phantom) polygonal knot population as a function of the number of edges. To assess the effect of knotting, we also determine the average values for polygons forming a given knot type as a function of the number of edges,

$$R^2(a,b,c) = \frac{a^2+b^2+c^2}{3}, \tag{1}$$

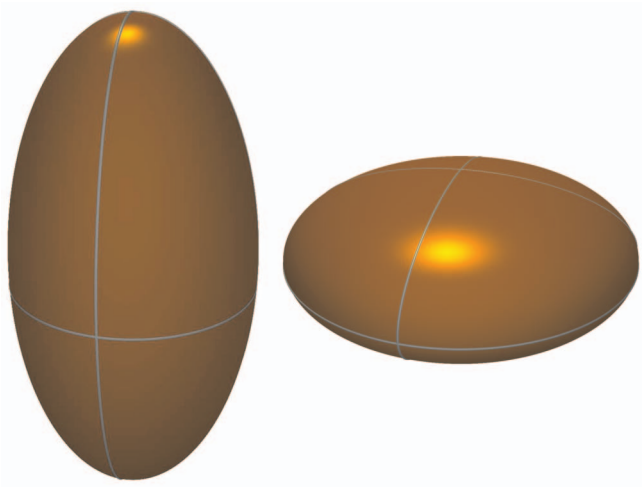

FIG. 1. (Color) Examples of a prolate (left) ellipsoid and an oblate (right) ellipsoid. One may think of the prolate ellipsoid as resembling a rugby football while the oblate ellipsoid is similar to M&M candy. The semiaxis lengths of these ellipsoids are (1,0.5,0.5) and (1,1,0.4), respectively. The asphericity of both ellipsoids is 0.0625 while the prolateness values are +1 and −1, respectively.

$$A(a,b,c) = \frac{(a-b)^2+(a-c)^2+(b-c)^2}{2(a+b+c)^2}, \tag{2}$$

$$P(a,b,c) = \frac{(2a-b-c)(2b-a-c)(2c-a-b)}{2(a^2+b^2+c^2-ab-ac-bc)^{3/2}}. \tag{3}$$

To appreciate the information carried by the asphericity, whose values range from 0 (meaning spherical) to 1 (meaning rodlike), and prolateness, whose values range from −1 (for perfectly oblate shapes, i.e., $a=b>c$) to +1 (for perfectly prolate shapes, i.e., $a>b=c$), it may be helpful to consider the examples shown in Fig. 1.

To test the effect of knotting on the shape of a frozen polymeric conformation, we must sort the freely jointed isosegmental polygonal models according to their topological knot type. When a random isosegmental polygon has three, four, or five edges, it is topologically equivalent to the standard regular polygon, i.e., it is an *unknot*, which is the designation of a polygon that is topologically equivalent to a standard circle. With six edges, one can form the first nontrivial knot, the *trefoil knot*, identified in standard knot tables as 3_1. For increasing numbers of edges, more and more different (and more complex) types of knots become possible (see Refs. 42–44 for a discussion of the equilateral polygons with the fewest number of edges for each knot type). The probability of obtaining a knotted polymer tends to one[45–47] as the number of edges approaches infinity. Furthermore, the availability of increasingly complex knotting with increasing numbers of edges has a significant impact on the average characteristics of random collections of freely jointed isosegmental polygons as a function of the number of edges.[12,13,15,16,48]

In Fig. 2 we show examples of enveloping and characteristic inertial ellipsoids for 50 edge trefoil knots with high, medium, and low asphericity values. An inspection of these examples shows that as expected, the enveloping ellipsoids are larger than the characteristic inertial ellipsoids and that

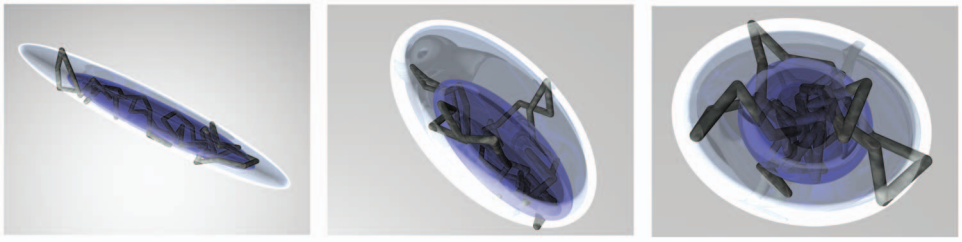

FIG. 2. (Color) Examples of 50 edge polygonal trefoil knots with high, medium, and low asphericity shown with their associated characteristic inertial ellipsoids and enveloping ellipsoids.

the centers of the enveloping and inertial ellipsoids are separated by distances that depend upon the specific instance. The examples also suggest that although the sizes and shapes of the inertial and enveloping ellipsoids, for a given polymer configuration, differ from each other to some extent, one should anticipate a correlation between the two measures of asphericity and prolateness, i.e., a chain whose shape is described by a prolate characteristic inertial ellipsoid is likely to fit into a prolate enveloping ellipsoid.

III. COMPUTATIONS

We have generated and analyzed freely jointed equilateral random polygons with 6–48 edges, with step size 2, and from 50 to 500 edges, with step size of 10 edges. For each number of edges, 400 000 random polygons were created using the hedgehog method.[49] This set of random knots was also used in Refs. 15, 16, and 50. To identify the knot type of each of the polygons, we use the HOMFLY polynomial[51] program of Ewing and Millett.[52] For each of the polygons, we determine the enveloping ellipsoid of smallest volume using the algorithm of Schonherr.[34] Using the resulting semiaxis lengths, we calculate the associated "radius of gyration" as well as the enveloping asphericity and prolateness for each of the random polygons using formulas 1–3. We then determine the average values for the knots 0_1, 3_1, 4_1, 5_1, 5_2, 6_1, 6_2, and 6_3 and for the entire knot population (i.e., phantom polygons) for each number of edges.

IV. RESULTS

The measures of inertial and enveloping scale and shape developed in this study and our earlier one[16] now provide the means to assess the differences between the inertial and enveloping measures, their dependence upon knotting, why these differences arise, and what they tell us about the physical properties of polymers. We first look at the question of scale.

A. The effect of topology on the scaling of polymers

Formula 1 allows us to determine the mean squared radius of gyration and the analogous quantity for enveloping ellipsoids to characterize the inertial and enveloping scale as a function of the number of edges. Classically, the mean squared radius of gyration is defined in inertial terms for objects composed of points with equal mass. It is equal to the mean square distance of these points from the center of mass of the object and can be expressed as the sum of the eigenvalues of the moment of inertial tensor. The classical inertial radius of gyration (denoted R_I) and squared radius of gyration (denoted R_I^2) are accepted measures of the overall size of polymers. They are used in studies of polymer scaling such as the effect of the chain length on the overall dimension of polymer chains.[11,24,53–55] Numerous theoretical and experimental studies have established that depending on the solvent quality, R_I scales with three different values determined by the critical exponent: $\nu=1/3$ for polymers suspended in a poor solvent where the polymer segments attract each other; $\nu=0.5$ for polymers in Θ conditions where the independent segments neither attract nor repel each other; and ν is approximately 0.588 for polymers in good solvents where the segments repel each other.[56] Interestingly, this simple rule changes when the topology is taken into account. When cyclic polymers, suspended in solvent under Θ conditions, are permitted to freely change their topology (such as in the case of DNA rings in the presence of certain types of topoisomerases), the scaling of the average size as a function of the chain length (without taking into account their actual topology) is characterized by the expected exponent, $\nu=0.5$. However, when cyclic polymers suspended in Θ conditions are divided into different knot types and one now calculates how the overall dimensions change for polymers of a given knot type, the scaling exponent changes to that of self-avoiding walks, ν becomes approximately 0.588.[8–16] It is important to stress here that the scaling exponent $\nu\approx0.588$ is not the effective exponent in the tested region but the real scaling exponent for very long polygons. It is not the consequence of knotting that increases the scaling exponent from 0.5 to 0.588 but the fact that the topology cannot change as the polygon increases in length. This is best exemplified by the simulations and theoretical treatment for scaling exponents of unknotted polygons with an effective diameter of zero.[8–16] This effect is clearly visible in Fig. 3 where we plot the effect of the chain length on R_I^2. The values of R_I^2 for phantom polymers (consisting of all accessible topological states) shows a linear scaling, i.e., twice ν or equal to 1.0. Profiles for the individual knot types exhibit a scaling of twice ν, approximately equal to 1.176. We also see that for the same chain size, the more complex knots show a smaller average R_I^2 in comparison to less complex knots.

Applying formula 1 to the enveloping measures of polymers defines a new measure of scale characterizing the size of the object in a manner analogous to the squared radius of gyration. This new enveloping scale measure (denoted R_E^2) is not a standard measure of polymer size although the enveloping ellipsoids have been used in many contexts to characterize shapes across many scales.[18–22,27,36–38] It is interesting to investigate whether R_E^2 scales in the same way as R_I^2, i.e., if they measure the scaling of polymers in the same manner. Figure 3 shows that this is indeed the case. The profiles of the phantom polygons for R_E^2 indicate a scaling exponent of

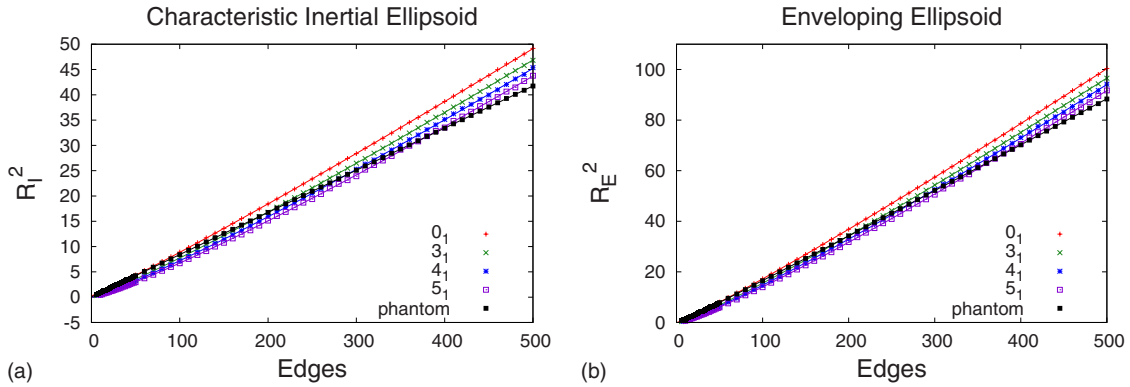

FIG. 3. (Color online) Mean values of inertial (left) and enveloping (right) squared radius of gyration calculated for random polygons with increasing numbers of segments and forming distinct knot types.

twice $\nu=0.5$, while the profiles of polygons with fixed knot type are very well fitted with a scaling exponent of twice $\nu=0.588$. Similar to R_I^2, the R_E^2 measures have the property that for the same number of segments, more complex knots are smaller than less complex knots. Of course, the R_E^2 values are bigger than the R_I^2 values for the same category of polygons. We observe an approximately twofold difference, for a fixed number of edges (Fig. 3). For measures such as certain hydrodynamic or diffusion properties of compact macromolecules, proteins for example, the R_E^2 values have been shown to be more informative in comparison to the R_I^2 values.[18–21,27,37]

B. The effect of topology on the shape of polymers

Having analyzed the effects of topology on the overall size of knotted polygons, we next look at how the average shape of knotted polymers is affected by the type of knot they form. Formulas 2 and 3 are used to measure the spatial asymmetry of the analyzed configurations. The semiaxis lengths of inertial or enveloping ellipsoids determined by each of the polygonal configurations provide the respective arguments, a, b, and c. Formula 2 gives the primary measure of spatial asymmetry with values that range from 0 (for a sphere) to 1 (for a straight segment). When a, b, and c are the semiaxis lengths of the characteristic inertial ellipsoids, the asphericity they define will be called the inertial asphericity A_I. The corresponding evaluation using the semiaxis lengths of the enveloping ellipsoids defines the enveloping asphericity A_E. In Fig. 4, we compare the A_I and A_E values of the analyzed polygons with various chain size and topology. It is striking that the A_I values for chains longer than 50 segments are significantly larger than the A_E values. In addition, the A_I values increase with the chain size and approach their asymptotic value from below while the opposite is observed for A_E values. In both cases we observe that for the same chain size, the more complex knots are more spherical than less complex polygons. For shorter chain length, in both cases the asphericity of phantom polymers is close to the values of the simplest knots. However, when complex knots begin to occur in greater numbers (with increasing chain size), the asphericity of the phantom polygons is closer to the asphericity values of the complex knots. This behavior for phantom polymers is explained by the fact that for short chain sizes, the most frequent knots are the simple knots and these are the dominant population within the set of the phantom chains. For long chain size, the situation changes as more complex knots start to dominate due to the exponentially increasing number of distinct topological types, even though the individual knot types are relatively rare.

We next describe why, for a given set of random polygons, the inertial asphericity values are significantly larger

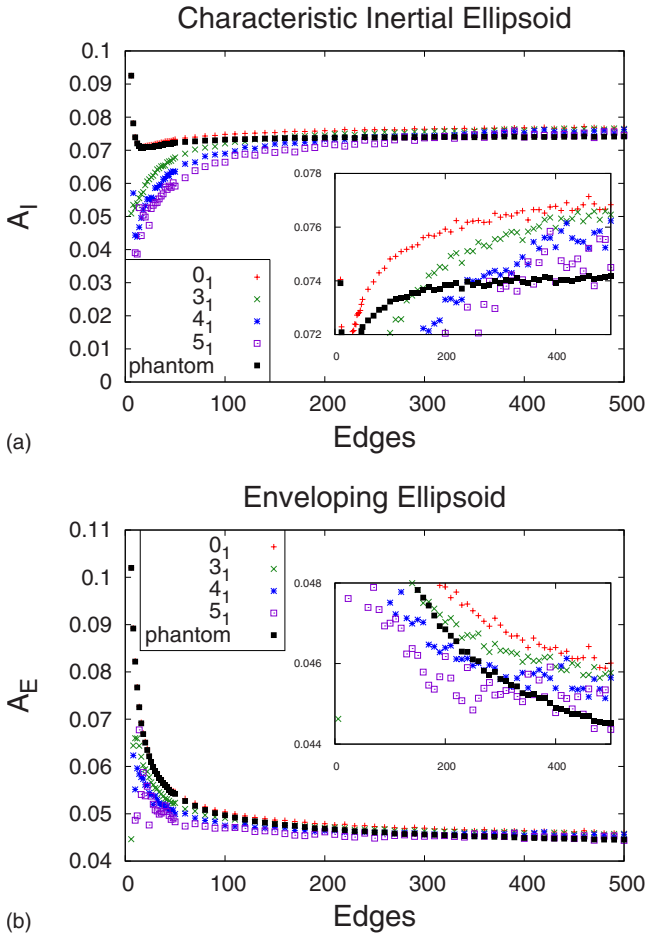

FIG. 4. (Color online) Mean values of inertial (top) and enveloping (bottom) asphericity calculated for random polygons with increasing numbers of segments and forming distinct knot types. The insets provide zoomed in views, permitting better differentiation between polygons forming the different knot types.

than the enveloping asphericity values, i.e., why, for a given knot type and number of edges, the enveloping ellipsoids are more spherical than the inertial ellipsoids. The reason is due to the anisotropic mass distribution within each random chain. Several studies have established that for long chains the mass distribution along the principal axis of gyration (the axis corresponding to the largest eigenvalue) of a momentary configuration of a random chain is either very flat or even bimodal (with a local minimum in the center) while the mass distribution along the remaining two principal axes of gyration has a Gaussian character.[18,20,57,58] This mass distribution causes the inertial ellipsoids of the momentary configurations of random chains and random polygons to be more aspherical than their corresponding enveloping ellipsoids. In this same way, a solid dumbbell is inertially more aspherical than its associated enveloping ellipsoid.

There is another striking difference between inertial and enveloping asphericity that is worthy of analysis. The enveloping asphericity values, on average, diminish with increasing number of edges in the random polygons and approach the asymptotic value of the asphericity, for a given knot type, from above. The opposite behavior is observed for the inertial asphericity. Why does this occur? In considering this effect, it is helpful to recall that the enveloping asphericity is determined by the position of only a relatively small number of external vertices of a given polygonal configuration while all the vertices, and the distribution of their locations, determine the inertial asphericity. Studies of the mass distribution within random chains and polygons reveal that, for relatively short chains, the mass distribution along the three principal axes of rotation is Gaussian. When the chains become longer, as noted above, a non-Gaussian distribution of mass is observed along the principal axis of rotation. This flat, non-Gaussian, character becomes more pronounced before stabilizing for long chains or polygons.[18,20,57,58] This behavior explains, therefore, why the inertial asphericity grows with the chain size of the analyzed random chains.

Why then does the enveloping asphericity decrease with the number of edges even though both the enveloping and the inertial asphericity values show that for a given number of edges, more complex knots are more spherical than less complex ones? We propose that this is because the enveloping ellipsoids are determined by a relatively small number of external points of the stochastic polygons. They act in a manner analogous to noise added to the real signal. To illustrate what we intend by this effect, consider a sphere with several randomly placed spikes, of limited height, on its surface. While the height of these spikes is random, suppose that it does not exceed a given bounding value. For a small sphere, such spikes would introduce significant enveloping asphericity in comparison to the scale of the sphere. However, as the sphere gets bigger, the spikes would have smaller and smaller effect, proportionally due to their limited height, i.e., the enveloping shape would become proportionally more spherical. We suggest that a similar effect causes the enveloping asphericity to be relatively large for small polygons and then decreases asymptotically to a characteristic value for polygons with a large number of edges. This effect would

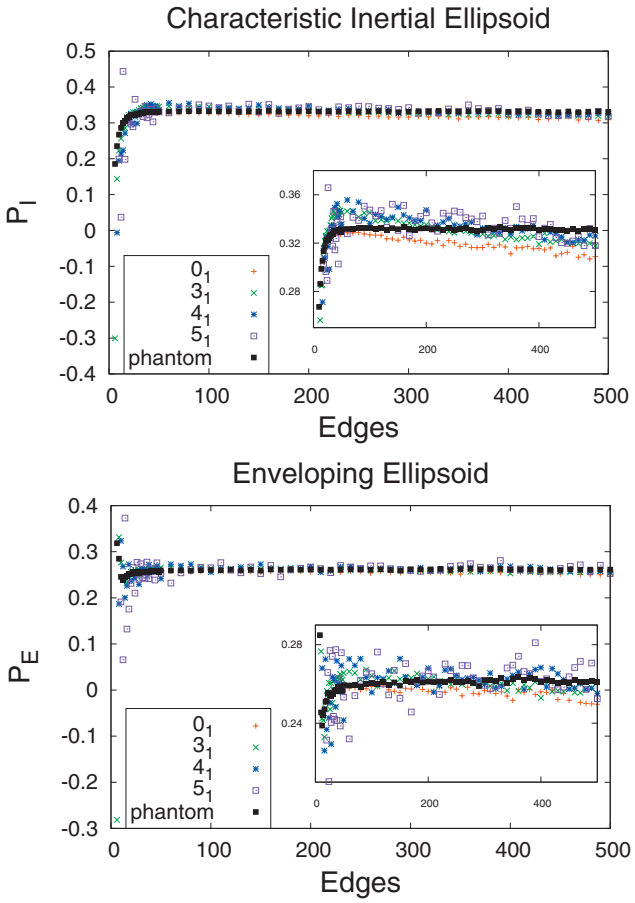

FIG. 5. (Color) Mean values of inertial (top) and enveloping (bottom) prolateness calculated for random polygons with increasing numbers of segments and forming distinct knot types. The insets provide zoomed in views, permitting better differentiation between polygons forming different knot types.

be insensitive to the fact that the mass distribution within random walks and polygons becomes more asymmetrical as the chain size increases.

The asphericity value tells us how much the object deviates from the sphere but it does not inform us whether the sphere is stretched, forming a prolate ellipsoid, resembling a rugby football, or whether the sphere is squeezed, forming an oblate ellipsoid, resembling an M&M candy or a pumpkin. To distinguish between these two cases another measure of spatial asymmetry was introduced[40,41] as expressed by formula 3. Since this measure has positive values for prolate ellipsoids and negative for oblate ones, we call this measure the prolateness of the conformation. The possible values of prolateness range from +1 for perfectly prolate ellipsoids ($a>b=c$) to −1 for perfectly oblate ellipsoids ($a=b>c$). In analogy to asphericity, we distinguish between inertial prolateness P_I and enveloping prolateness P_E. Figure 5 shows the dependence of the P_I and P_E values of the polygons as a function of the chain size and topology. We observe that P_I has significantly higher values than P_E. As above, we propose that this reflects the anisotropy of mass distribution along the longest axis of the inertial ellipsoid. Thus, if the object is prolate, one would expect that its P_I value would be bigger than the corresponding P_E value. Both P_I and P_E show that more complex knots are more prolate than less

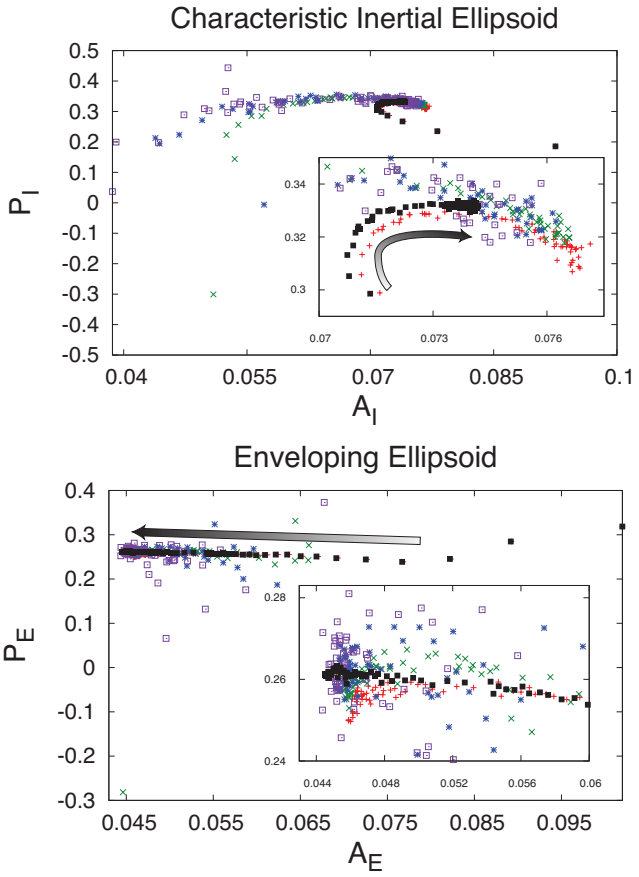

FIG. 6. (Color) Changes in asphericity and prolateness based on inertial (top) and enveloping (bottom) measures for random polygons with increasing numbers of segments and forming distinct knot types. The arrows indicate the progression direction resulting from increasing the number of segments in polygons within a given knot type.

complex knots for the same number of segments. This observation may seem to contradict the data presented in Fig. 4. There we see that for the same number of segments, more complex knots have more spherical shapes than less complex knots. However, there is no real contradiction as the flattening of prolate shapes from the sides decreases their prolateness but can increase the asphericity. This is illustrated in Fig. 1, where we hold the asphericity constant while changing the prolateness, showing that the asphericity and prolateness are not correlated with each other. Thus, the overall shapes of more complex knots are closer to the shape of a well inflated rugby football while the shape of less complex knots resembles more closely that of an underinflated rugby football.

C. The influence of knotting on the joint evolution of asphericity and prolateness of polymers

Figure 6 presents a new perspective on the evolution of shapes of random polygons that form the various knot types. By plotting prolateness versus asphericity and by indicating the direction corresponding to the increase in the number of edges of the random polygons, we can better appreciate the differences and similarities between inertial and enveloping measures of polymer shape. As we have already discussed the differences, we now focus on the similarities. In both cases, phantom chains tend to different limiting values than individual knot types. While limiting values for inertial and enveloping measures are different from each other, the individual knot types seem to converge to the same universal value for a given measure. Table I shows that the statistically estimated limiting asphericity values determined using the Monte Carlo Markov chain analysis described in Ref. 16. From Fig. 6 one gains a greater sense of the dynamics of this evolution and one can observe the convergence process in a compelling manner. The explanation of this convergent behavior lies, we propose, in the phenomenon of knot localization.[53,59,60] Although the presence of local and global knots occur with probability approaching one as the number of edges goes to infinity,[45,46,61,62] several papers have established that for long chains, on average, knots tend to be localized.[63–66] This implies that the average length of the knotted portion becomes shorter and shorter in relation to the entire polygon as the number of edges increases. As a consequence, for very long chains, the shape differences between polygons that are unknotted or those that form simple prime knots should become less and less significant. Figure 6 clearly shows just such an evolution of the shape parameters. Why then do the phantom polygon shape parameters tend to distinctly different values? The answer lies in the fact that phantom chains increase their average knottedness, i.e., acquire more and more complex knots at an exponential rate, with increasing number of edges. These more complex knots require much longer chain size for their formation. Thus, the phantom polygons acquire so many more complex knots that their average asphericity and prolateness parameters never converge to those of the unknot. Note, however, that the average shape of phantom polygons shows a convergence to limiting values for asphericity and prolateness.

TABLE I. Estimation of the asymptotic enveloping asphericity and inertial asphericity values.

Knot	Enveloping asphericity	Inertial asphericity
Phantom	$0.040\,92 \pm 0.000\,28$	$0.074\,36 \pm 0.000\,42$
0_1	$0.043\,53 \pm 0.000\,48$	$0.078\,75 \pm 0.000\,75$
3_1	$0.044\,24 \pm 0.000\,63$	$0.079\,31 \pm 0.000\,10$
4_1	$0.044\,49 \pm 0.001\,42$	$0.079\,72 \pm 0.002\,08$
5_1	$0.046\,12 \pm 0.002\,41$	$0.081\,37 \pm 0.003\,70$
5_2	$0.045\,50 \pm 0.001\,84$	$0.081\,90 \pm 0.002\,86$
6_1	$0.046\,67 \pm 0.003\,52$	$0.085\,34 \pm 0.005\,46$
6_2	$0.044\,56 \pm 0.003\,25$	$0.080\,65 \pm 0.005\,14$
6_3	$0.043\,03 \pm 0.004\,21$	$0.078\,25 \pm 0.006\,33$

D. The effect of topology on scale and shape of knotted polymers

In Fig. 7 we compare the inertial and enveloping ellipsoidal shapes reflecting the average size and shape of several simple polygonal knot types with 500 segments. Here we can observe that the enveloping ellipsoids are bigger (as naturally expected) and that they are more spherical. Focusing on similarities between the inertial and enveloping measures, one notices that the order in which each of the ellipsoids are nested is the same in both cases, i.e., 0_1, 3_1, 4_1, and phantom

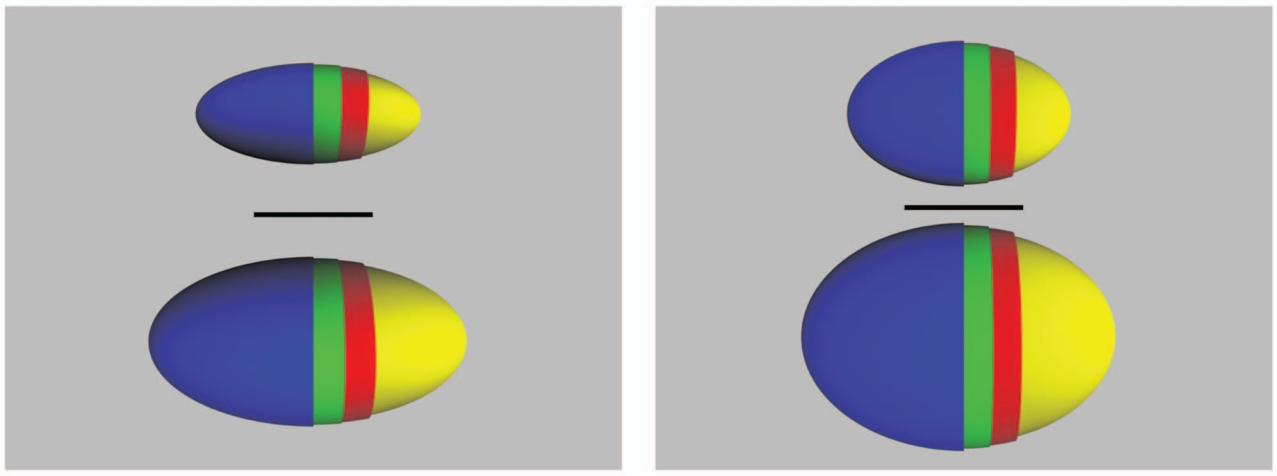

FIG. 7. (Color) Average sizes and shapes of characteristic inertial (top) and enveloping (bottom) ellipsoids representing 500 segment polygons forming 0_1 knots (blue), 3_1 knots (green), 4_1 knots (red), and phantom polygons (yellow). The ellipsoids are seen along the middle (left) and shortest (right) axes of inertia. The black bar represents the size of ten statistical segments.

chains, in order of decreasing size. It would be interesting to know whether this order of nesting is universal and whether every pair of knots would follow the same nesting order according to inertial and enveloping measures of polymer shape for all polymer lengths.

V. CONCLUSIONS

Whereas it is well known that the overall inertial and enveloping shape of momentary configurations of linear and cyclic polymers at thermal equilibrium can be approximated by prolate ellipsoids, the extent to which the asymmetry of those ellipsoids depends on knotting has not been investigated. Nor has the distinct differences between inertial and enveloping measures of shape been described. We have compared these inertial and enveloping measures of anisotropy and observed that the inertial measures of random polygons give higher asphericity in comparison to the enveloping measures. We propose that the enveloping measures of spatial asymmetry are distinctly different reporters of polymer shape compared to the inertial measures. We observe, however, that the two measures are correlated and both reveal, for example, that polygons forming more complex knots are more spherical and more prolate than polygons forming less complex knots with the same number of segments.

ACKNOWLEDGMENTS

The authors wish to thank John Kern for his statistical advice during the course of this research. K.C.M., E.J.R., and A.S. wish to thank the Institute for Mathematics and its Applications (Minneapolis, MN, USA with funds provided from the National Science Foundation) for support during the thematic year: Mathematics of Molecular and Cellular Biology. K.C.M. also thanks the Centre de Mathematiques et d'Informatique (Marseille, France) and the Centre de Mathematiques du Luberon (Grambois, France) for their hospitality during this work. A.S. was supported in part by the Swiss National Science Foundation under Grant No. 3100A0-116275. E.J.R. was supported in part by the National Science Foundation under Grant No. DMS0810415.

[1] A. Vologodskii, A. Lukashin, M. Frank-Kamenetskii, and V. Anshelevich, Sov. Phys. JETP **39**, 1059 (1974).
[2] J. des Cloizeaux and M. Mehta, J. Phys. I (France) **40**, 665 (1979).
[3] J. P. J. Michels and F. W. Wiegel, Proc. R. Soc. London, Ser. A **403**, 269 (1986).
[4] K. Koniaris and M. Muthukumar, Phys. Rev. Lett. **66**, 2211 (1991).
[5] K. Koniaris and M. Muthukumar, J. Chem. Phys. **95**, 2873 (1991).
[6] T. Deguchi and K. Tsurusaki, J. Phys. Soc. Jpn. **62**, 1411 (1993).
[7] T. Deguchi and K. Tsurusaki, Phys. Rev. E **55**, 6245 (1997).
[8] J. M. Deutsch, Phys. Rev. E **59**, R2539 (1999).
[9] A. Y. Grosberg, Phys. Rev. Lett. **85**, 3858 (2000).
[10] N. T. Moore, R. C. Lua, and A. Y. Grosberg, Proc. Natl. Acad. Sci. U.S.A. **101**, 13431 (2004).
[11] M. K. Shimamura and T. Deguchi, Phys. Rev. E **65**, 051802 (2002).
[12] A. Dobay, J. Dubochet, K. Millett, P.-E. Sottas, and A. Stasiak, Proc. Natl. Acad. Sci. U.S.A. **100**, 5611 (2003).
[13] Y. Diao, A. Dobay, R. B. Kusner, K. C. Millett, and A. Stasiak, J. Phys. A **36**, 11561 (2003).
[14] K. Millett, A. Dobay, and A. Stasiak, Macromolecules **38**, 601 (2005).
[15] P. Plunkett, M. Piatek, A. Dobay, J. Kern, K. Millett, A. Stasiak, and E. Rawdon, Macromolecules **40**, 3860 (2007).
[16] E. J. Rawdon, J. C. Kern, M. Piatek, P. Plunkett, A. Stasiak, and K. C. Millett, Macromolecules **41**, 8281 (2008).
[17] W. Kuhn, Colloid Polym. Sci. **68**, 2 (1934).
[18] G. Wei and B. E. Eichinger, Macromolecules **22**, 3429 (1989).
[19] G. Wei and B. E. Eichinger, Macromolecules **23**, 4845 (1990).
[20] G. Wei, Macromolecules **30**, 2130 (1997).
[21] G. M. Sigalov, J. Ibuki, T. Chiba, and T. Inoue, Macromolecules **30**, 7759 (1997).
[22] C. Haber, S. A. Ruiz, and D. Wirtz, Proc. Natl. Acad. Sci. U.S.A. **97**, 10792 (2000).
[23] B. Maier and J. O. Rädler, Macromolecules **34**, 5723 (2001).
[24] G. Zifferer and W. Preusser, Macromol. Theory Simul. **10**, 397 (2001).
[25] L. Guo and E. Luijten, Macromolecules **36**, 8201 (2003).
[26] M. O. Steinhauser, J. Chem. Phys. **122**, 094901 (2005).
[27] Y. E. Ryabov, C. Geraghty, A. Varshey, and D. Fushman, J. Am. Chem. Soc. **128**, 15432 (2006).
[28] W. R. Taylor, J. M. Thornton, and W. G. Turnell, J. Mol. Graphics **1**, 30 (1983).
[29] W. R. Taylor and A. Aszodi, *Protein Geometry, Classification, Topology and Symmetry: A Computational Analysis of Structure*, Series in Biophysics (Taylor & Francis, New York, 2004).
[30] J. Rudnick and G. Gaspari, J. Phys. A **19**, L191 (1986).
[31] M. Bishop and J. P. J. Michels, J. Chem. Phys. **85**, 1074 (1986).

[32] M. Bishop and C. J. Saltiel, J. Chem. Phys. **88**, 3976 (1988).
[33] H. W. Diehl and E. Eisenriegler, J. Phys. A **22**, L87 (1989).
[34] S. Schonherr, Ph.D. thesis, Freie Universitat Berlin, 1994.
[35] J. R. Banavar, T. X. Hoang, A. Maritan, C. Poletto, A. Stasiak, and A. Trovato, Proc. Natl. Acad. Sci. U.S.A. **104**, 17283 (2007).
[36] N. Chugai and R. Chevalier, Astrophys. J. **657**, 378 (2007).
[37] A. Ozerin, A. Muzafarov, A. Kuklin, A. Islavov, V. Gordelyi, G. Ignat'eva, V. Myakushev, L. Ozerina, and E. Tatarinova, Dokl. Chem. **395**, 59 (2004).
[38] S. Hermes, M.-K. Schröter, R. Schmid, L. Khodeir, M. Muhler, A. Tissler, R. W. Fischer, and R. A. Fischer, Angew. Chem., Int. Ed. **44**, 6237 (2005).
[39] T. Cai, L. Xu, H. W. Gibson, H. C. Dorn, C. J. Chancellor, M. M. Olmstead, and A. L. Balch, J. Am. Chem. Soc. **129**, 10795 (2007).
[40] J. A. Aronovitz and D. R. Nelson, J. Phys. I (France) **47**, 1445 (1986).
[41] J. W. Cannon, J. A. Aronovitz, and P. Goldbart, J. Phys. I **1**, 629 (1991).
[42] K. C. Millett, *Random Knotting and Linking* (World Scientific, Singapore, 1994), pp. 31–46.
[43] J. A. Calvo and K. C. Millett, in *Ideal Knots*, Series in Knots Everything, Vol. 19 (World Scientific, River Edge, NJ, 1998), pp. 107–128.
[44] E. J. Rawdon and R. G. Scharein, *Physical Knots: Knotting, Linking, and Folding Geometric Objects in* $\mathbb{R}^3$, Contemporary Mathematics, Vol. 304 (American Mathematical Society, Providence, RI, 2002), pp. 55–75.
[45] D. W. Sumners and S. G. Whittington, J. Phys. A **21**, 1689 (1988).
[46] N. Pippenger, Discrete Appl. Math. **25**, 273 (1989).
[47] Y. Diao, J. Knot Theory Ramif. **4**, 189 (1995).
[48] E. Rawdon, A. Dobay, J. C. Kern, K. C. Millett, M. Piatek, P. Plunkett, and A. Stasiak, Macromolecules **41**, 4444 (2008).
[49] K. V. Klenin, A. V. Vologodskii, V. V. Anshelevich, A. M. Dykhne, and M. D. Frank-Kamenetskii, J. Biomol. Struct. Dyn. **5**, 1173 (1988).
[50] K. C. Millett, M. Piatek, and E. J. Rawdon, J. Knot Theory Ramif. **17**, 601 (2008).
[51] P. Freyd, D. Yetter, J. Hoste, W. B. R. Lickorish, K. Millett, and A. Ocneanu, Bull. Am. Math. Soc. **12**, 239 (1985).
[52] B. Ewing and K. C. Millett, *Progress in Knot Theory and Related Topics* (Hermann, Paris, 1997), pp. 51–68.
[53] E. J. Janse van Rensburg and S. G. Whittington, J. Phys. A **24**, 3935 (1991).
[54] M. Le Bret, Biopolymers **19**, 619 (1980).
[55] M. K. Shimamura and T. Deguchi, J. Phys. A **35**, L241 (2002).
[56] B. Li, N. Madras, and A. D. Sokal, J. Stat. Phys. **80**, 661 (1995).
[57] R. J. Rubin and J. Mazur, Macromolecules **10**, 139 (1977).
[58] D. N. Theodorou and U. W. Suter, Macromolecules **18**, 1206 (1985).
[59] E. Orlandini, M. C. Tesi, E. J. J. van Rensburg, and S. G. Whittington, J. Phys. A **29**, L299 (1996).
[60] E. Orlandini, M. Tesi, E. Janse van Rensburg, and S. Whittington, J. Phys. A **31**, 5953 (1998).
[61] Y. Diao, N. Pippenger, and D. W. Sumners, J. Knot Theory Ramif. **3**, 419 (1994).
[62] Y. Diao, J. C. Nardo, and Y. Sun, J. Knot Theory Ramif. **10**, 597 (2001).
[63] V. Katritch, W. K. Olson, A. Vologodskii, J. Dubochet, and A. Stasiak, Phys. Rev. E **61**, 5545 (2000).
[64] A. Dobay, P.-E. Sottas, J. Dubochet, and A. Stasiak, Lett. Math. Phys. **55**, 239 (2001).
[65] B. Marcone, E. Orlandini, A. L. Stella, and F. Zonta, J. Phys. A **38**, L15 (2005).
[66] P. Virnau, Y. Kantor, and M. Kardar, J. Am. Chem. Soc. **127**, 15102 (2005).